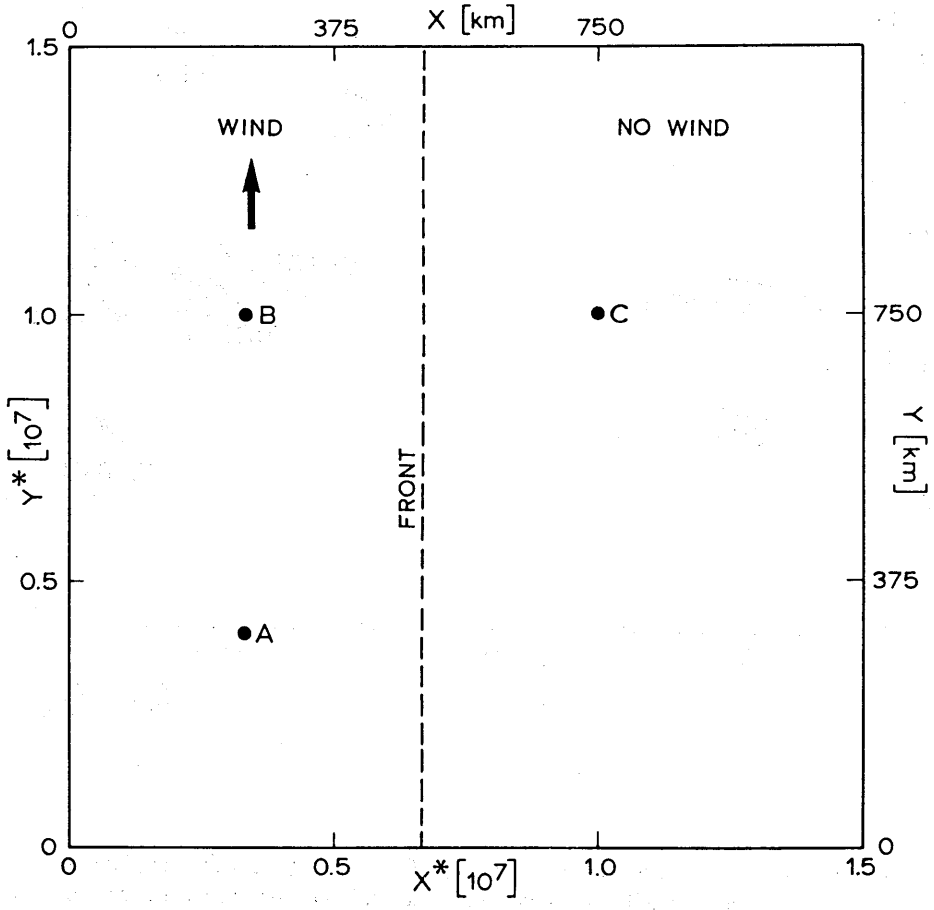

Fig. 50-9.1-0 Wind field geometry for Case IV. A,B and C denote special output points.

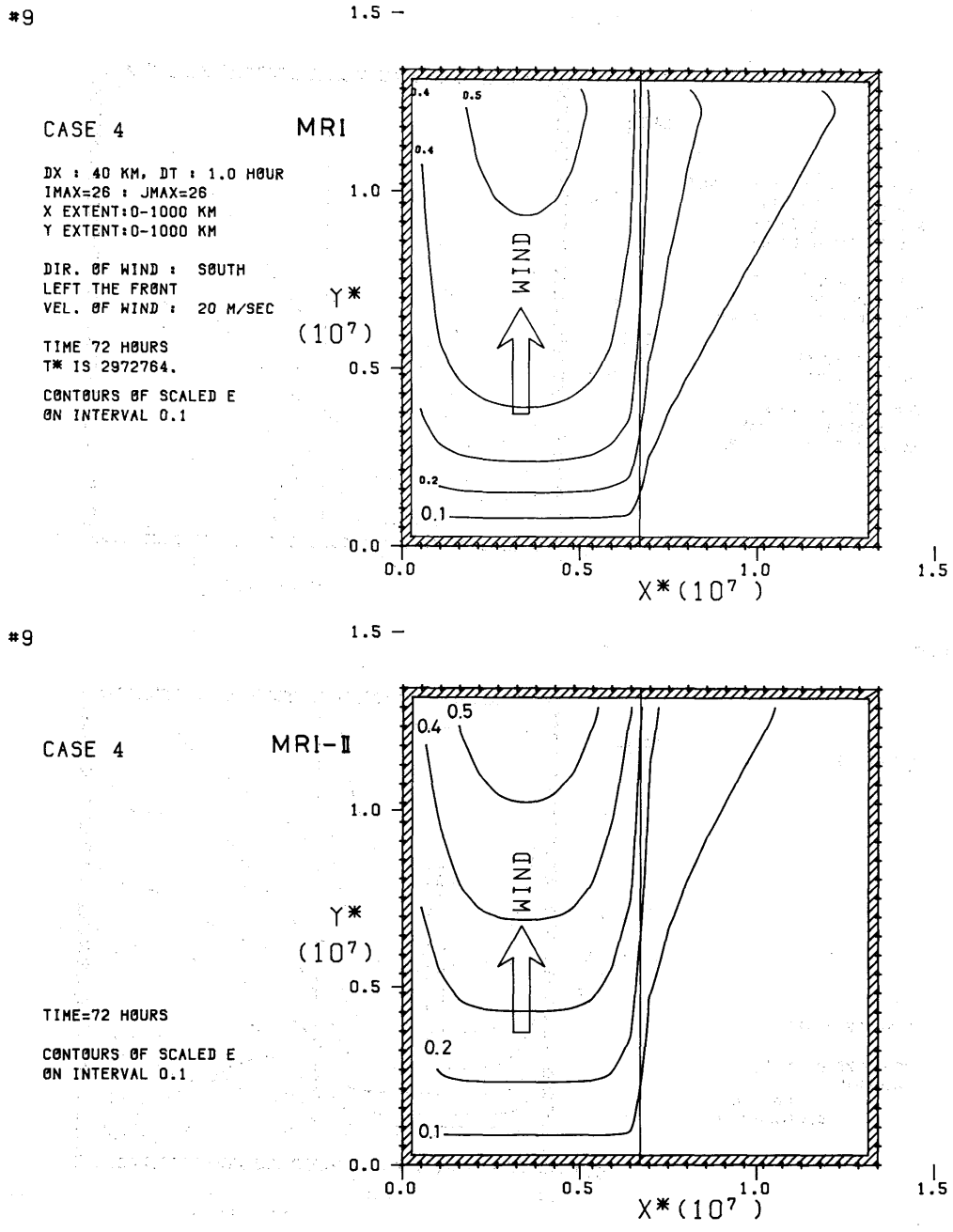

Fig. 51-0-18 countours of E/E_{PM} vs. X^* and Y^*

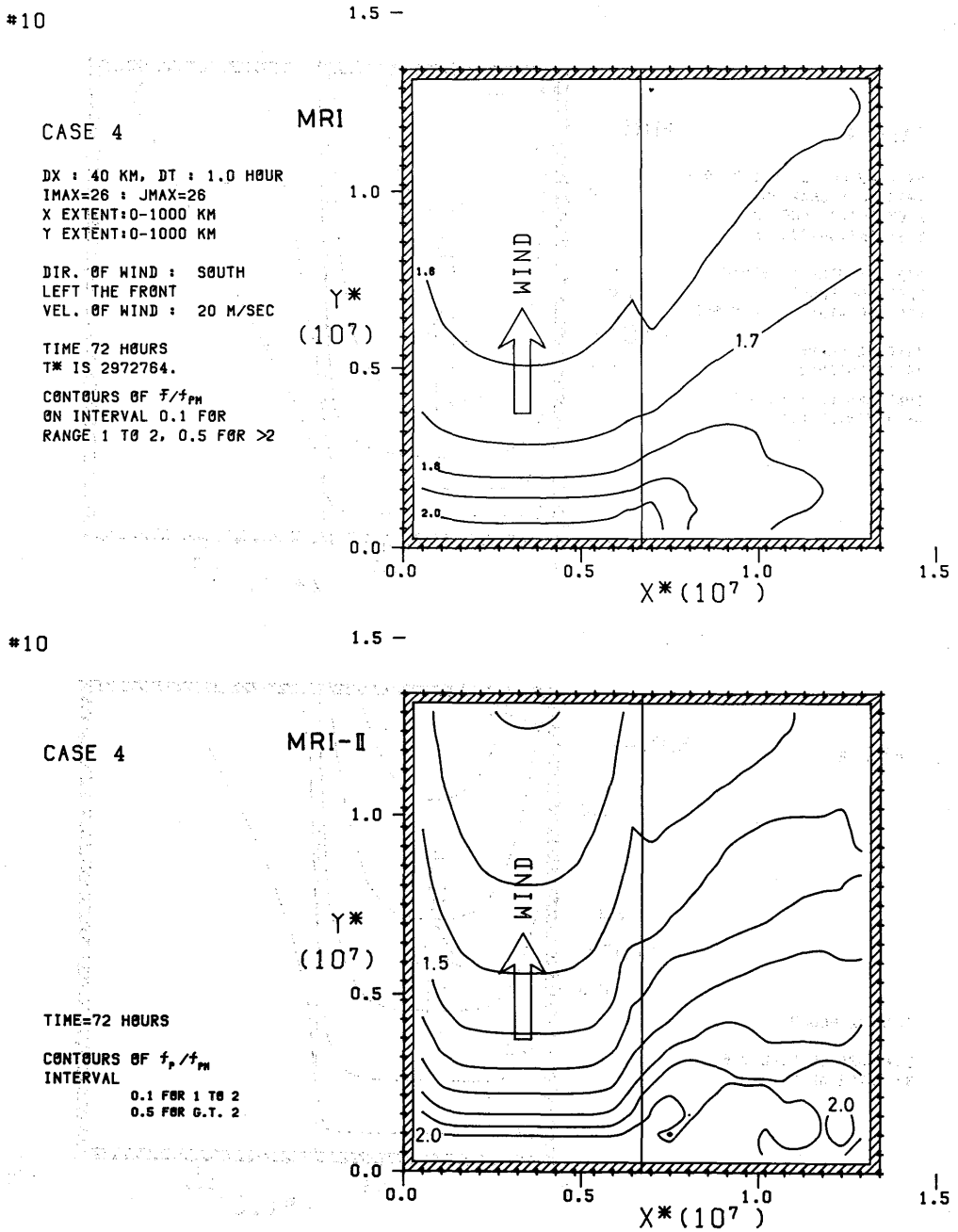

Fig. 52-0-19 countours of $\bar{f}/f_{PM}$ vs. X^* and Y^*

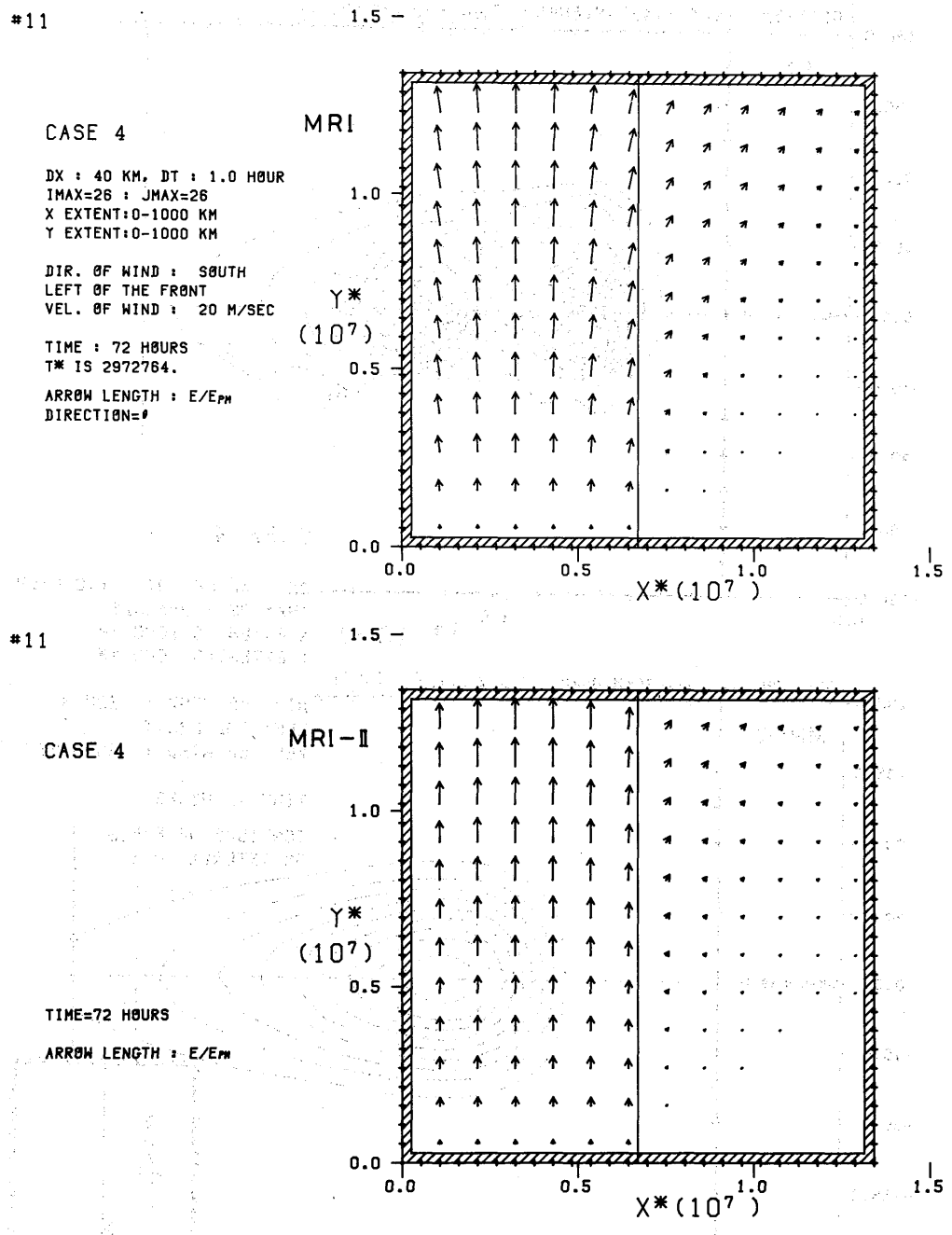

Fig. 53-9.2-20 custer diagram of E/E_{PM} and $\bar{\theta}$ vs. X^* and Y^*

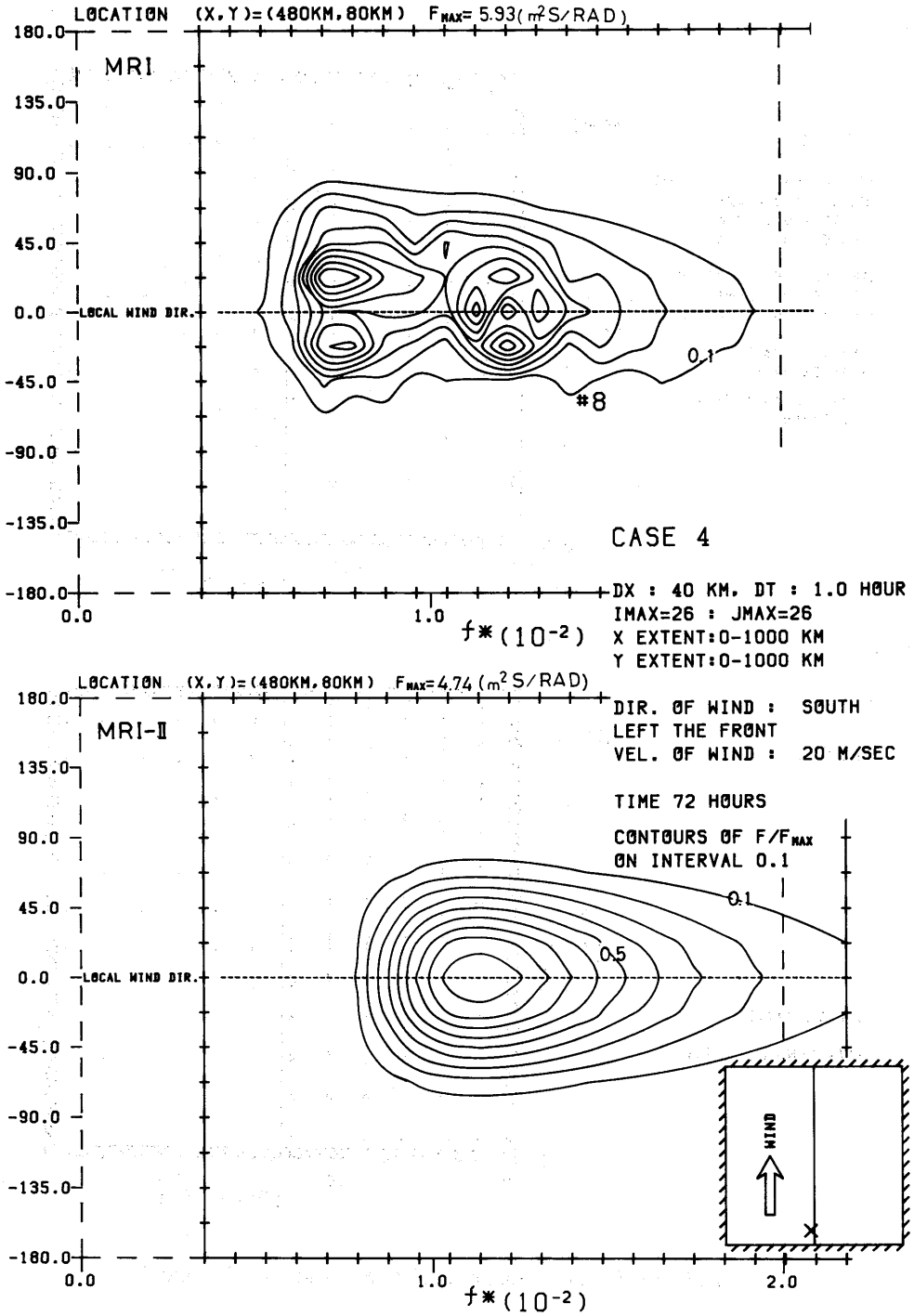

Fig. 54-0-0 scaled 2-D spectrum $F(f,\theta)/F(f,\theta)_{MAX}$ for $T = 72$ hrs and point (480,80)

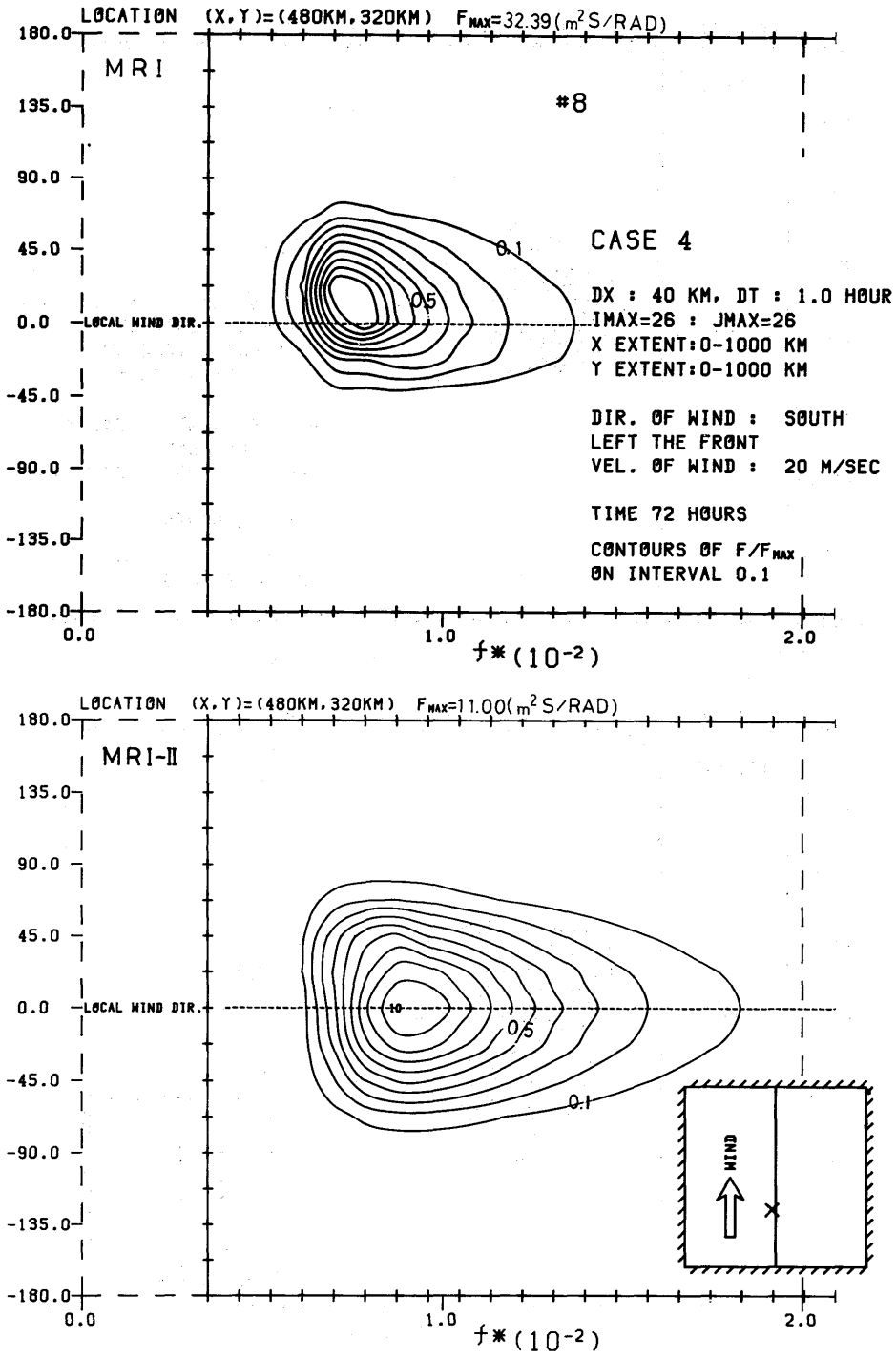

Fig. 55-0-21 scaled 2-D spectrum $F(f,\theta)/F(f,\theta)_{MAX}$ for $T = 72$ hrs and point (480,320)

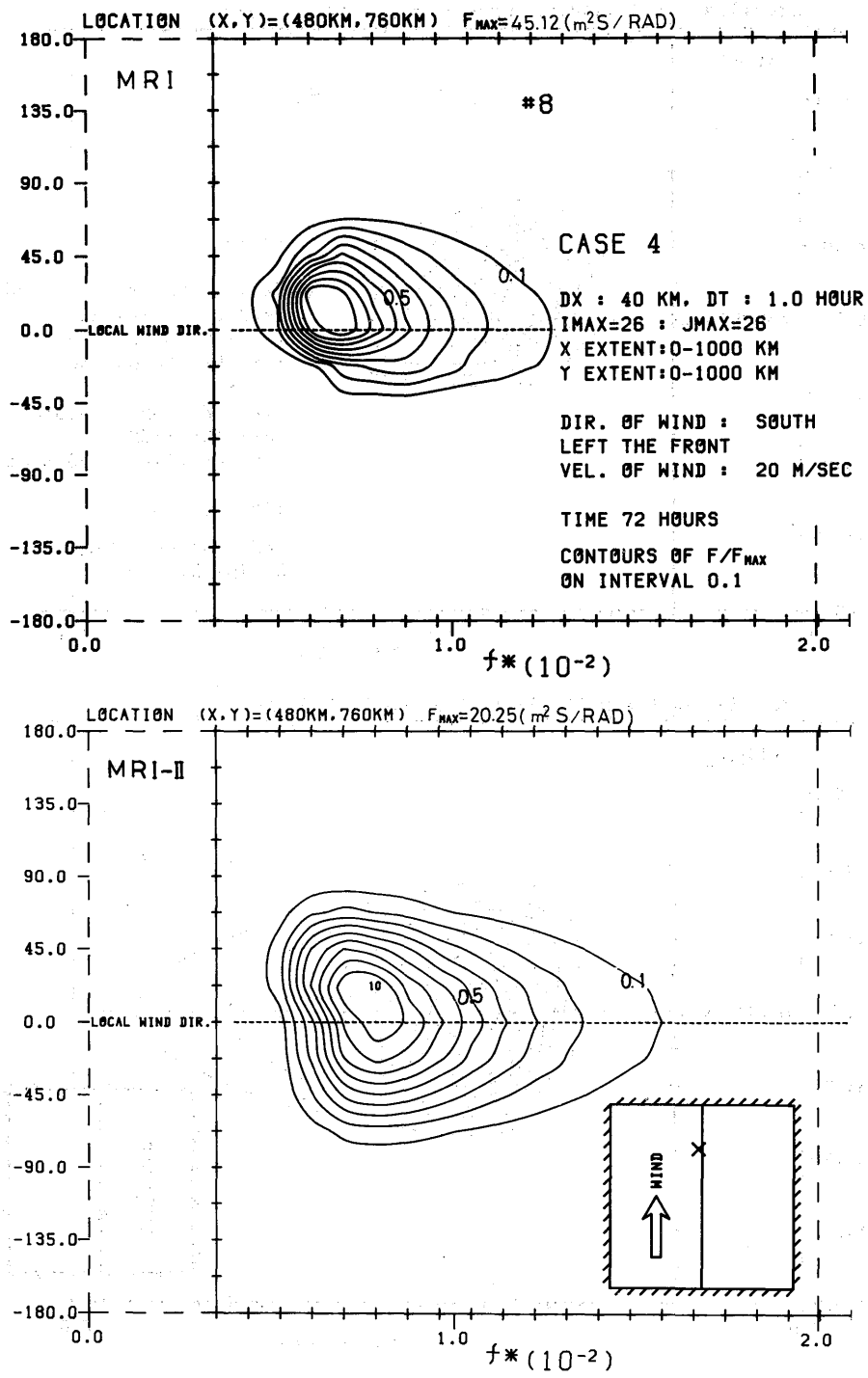

Fig. 56-0-0 scaled 2-D spectrum $F(f,\theta)/F(f,\theta)_{MAX}$ for T = 72 hrs and point (480,760)

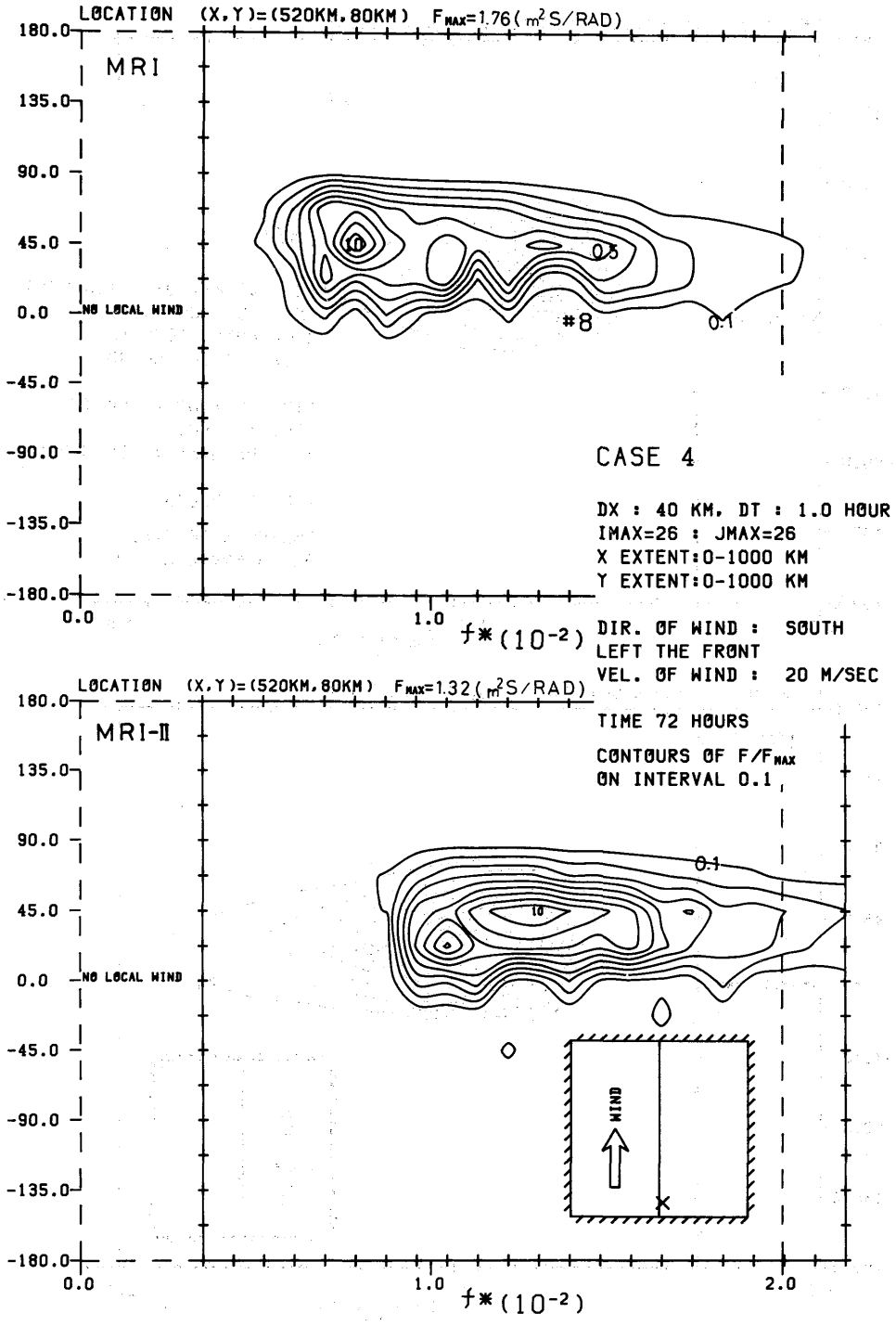

Fig. 57-0-0 scaled 2-D spectrum $F(f,\theta)/F(f,\theta)_{MAX}$ for T = 72 hrs and point (520,80)

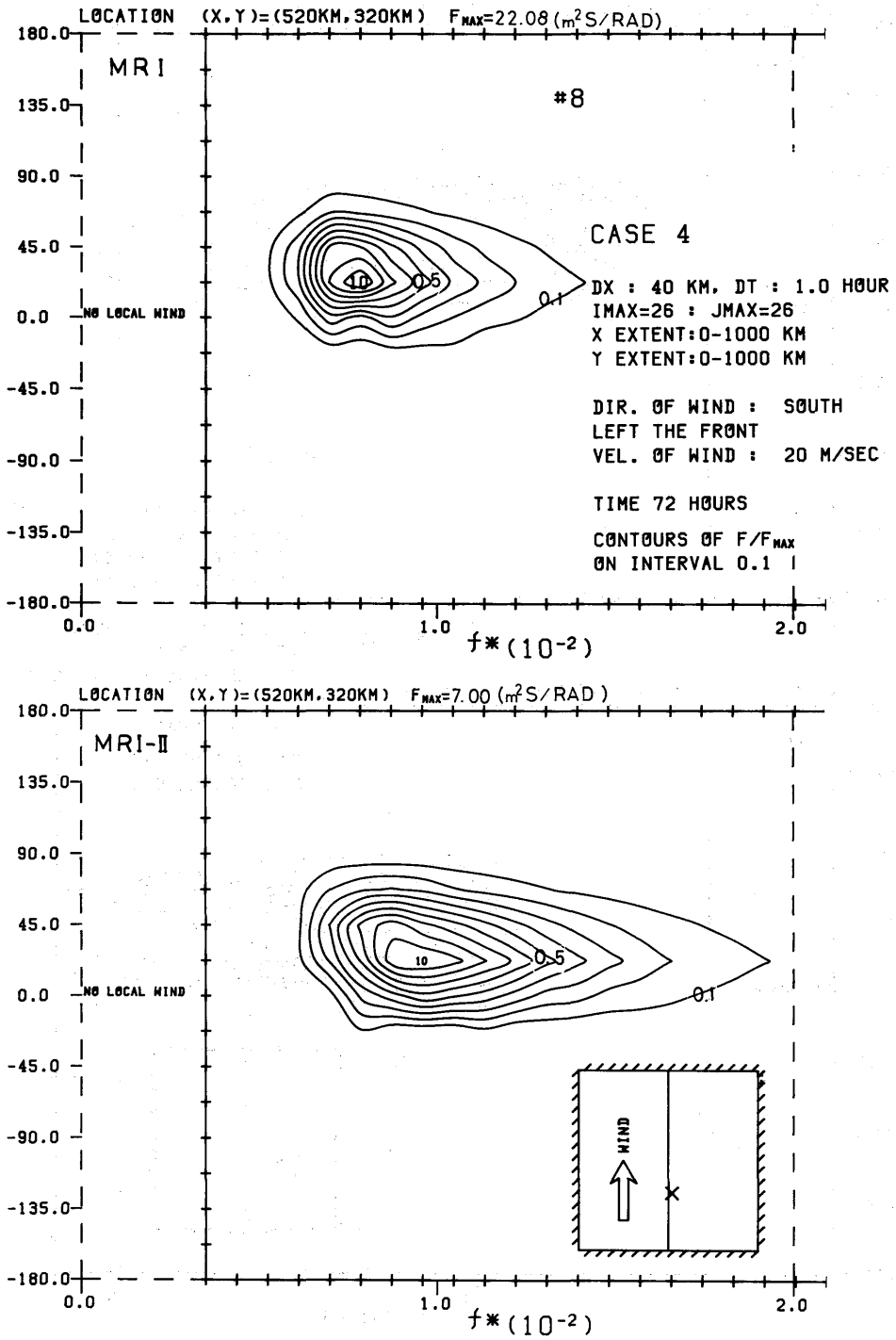

Fig. 58-0-22 scaled 2-D spectrum $F(f,\theta)/F(f,\theta)_{MAX}$ for $T = 72$ hrs and point (520,320)

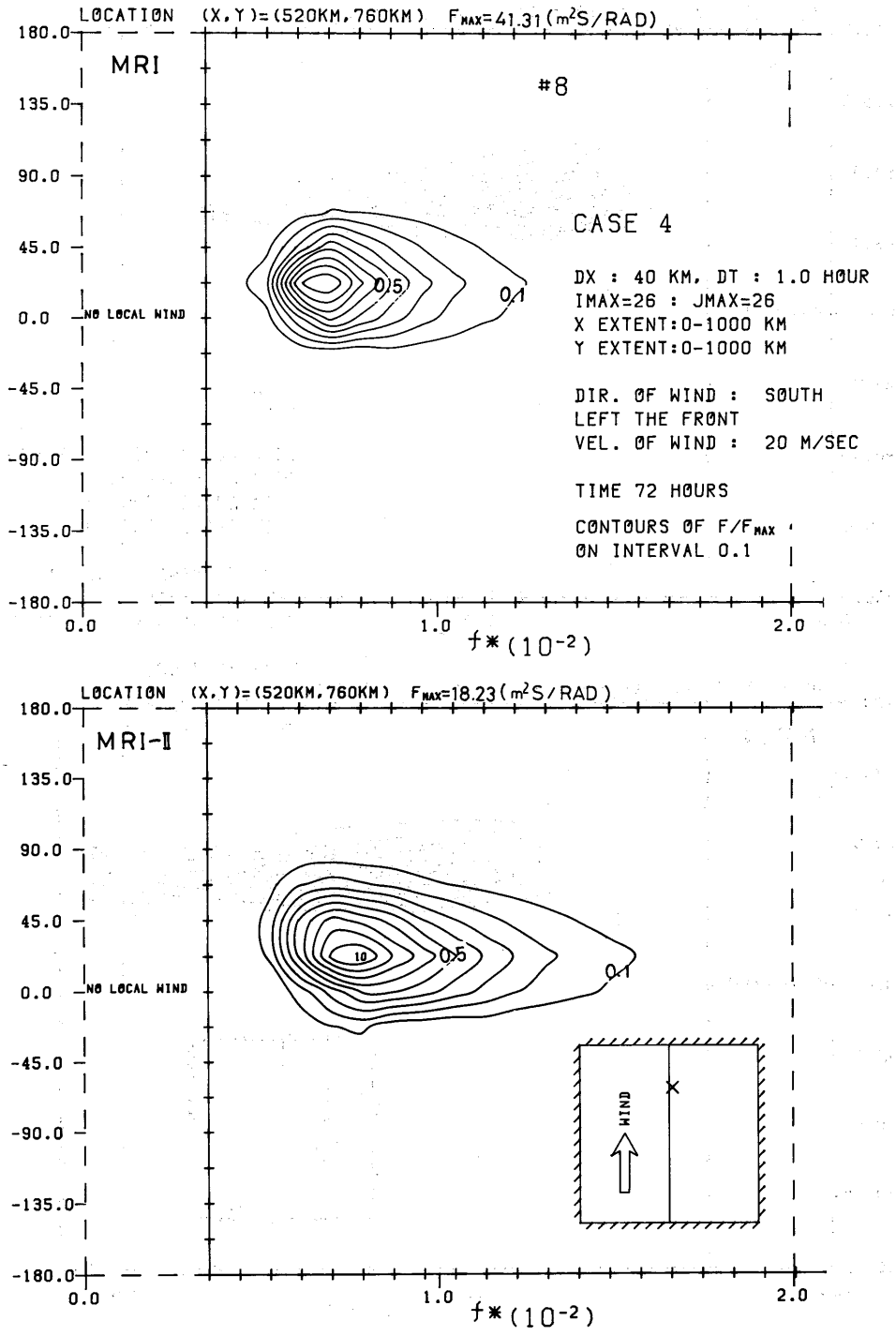

Fig. 59-0-0 scaled 2-D spectrum $F(f,\theta)/F(f,\theta)_{MAX}$ for $T = 72$ hrs and point (520,760)

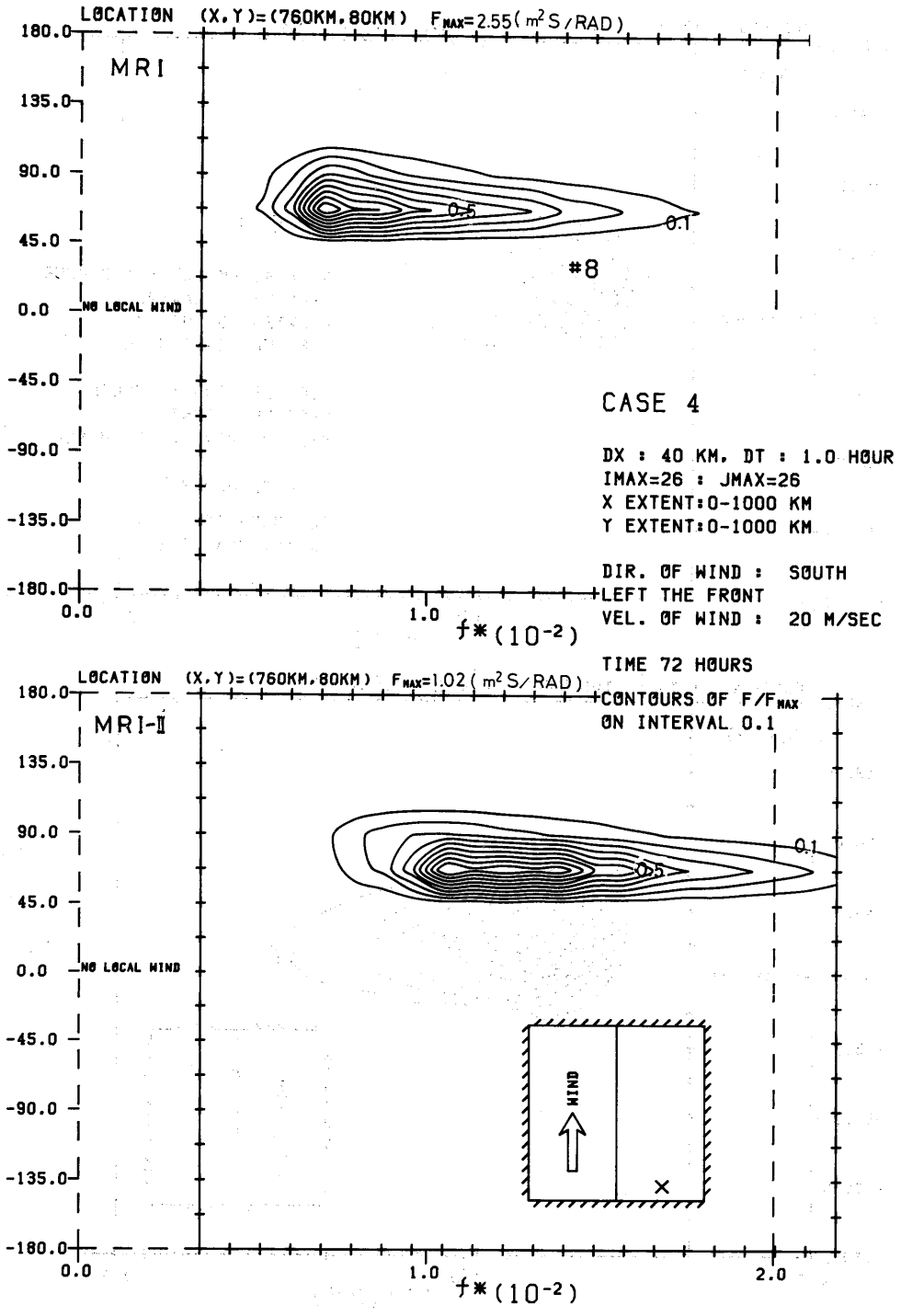

Fig. 60-0-0 scaled 2-D spectrum $F(f,\theta)/F(f,\theta)_{MAX}$ for T = 72 hrs and point (760,80)

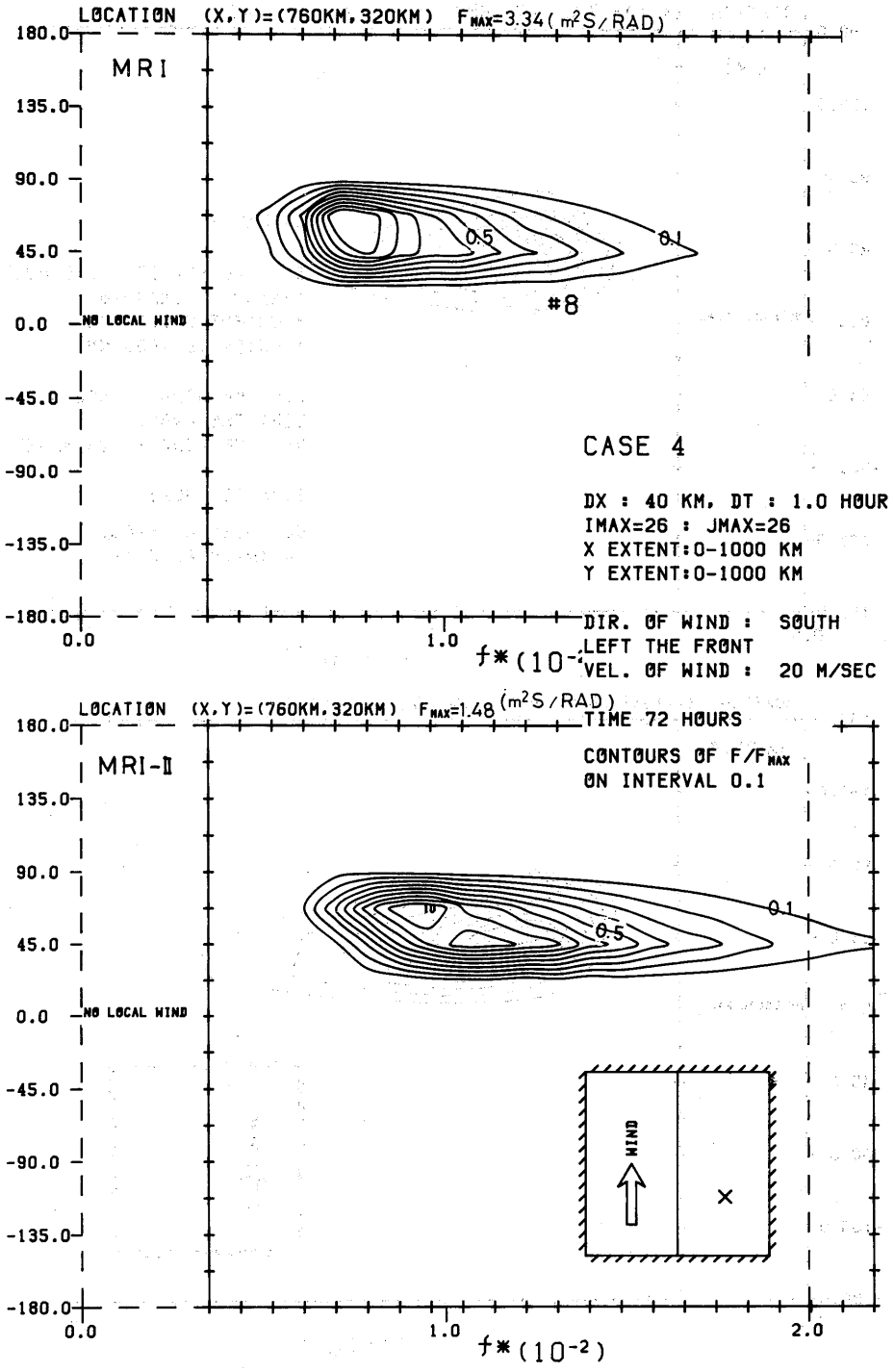

Fig. 61-0-0 scaled 2-D spectrum $F(f,\theta)/F(f,\theta)_{MAX}$ for T = 72 hrs and point (760,320)

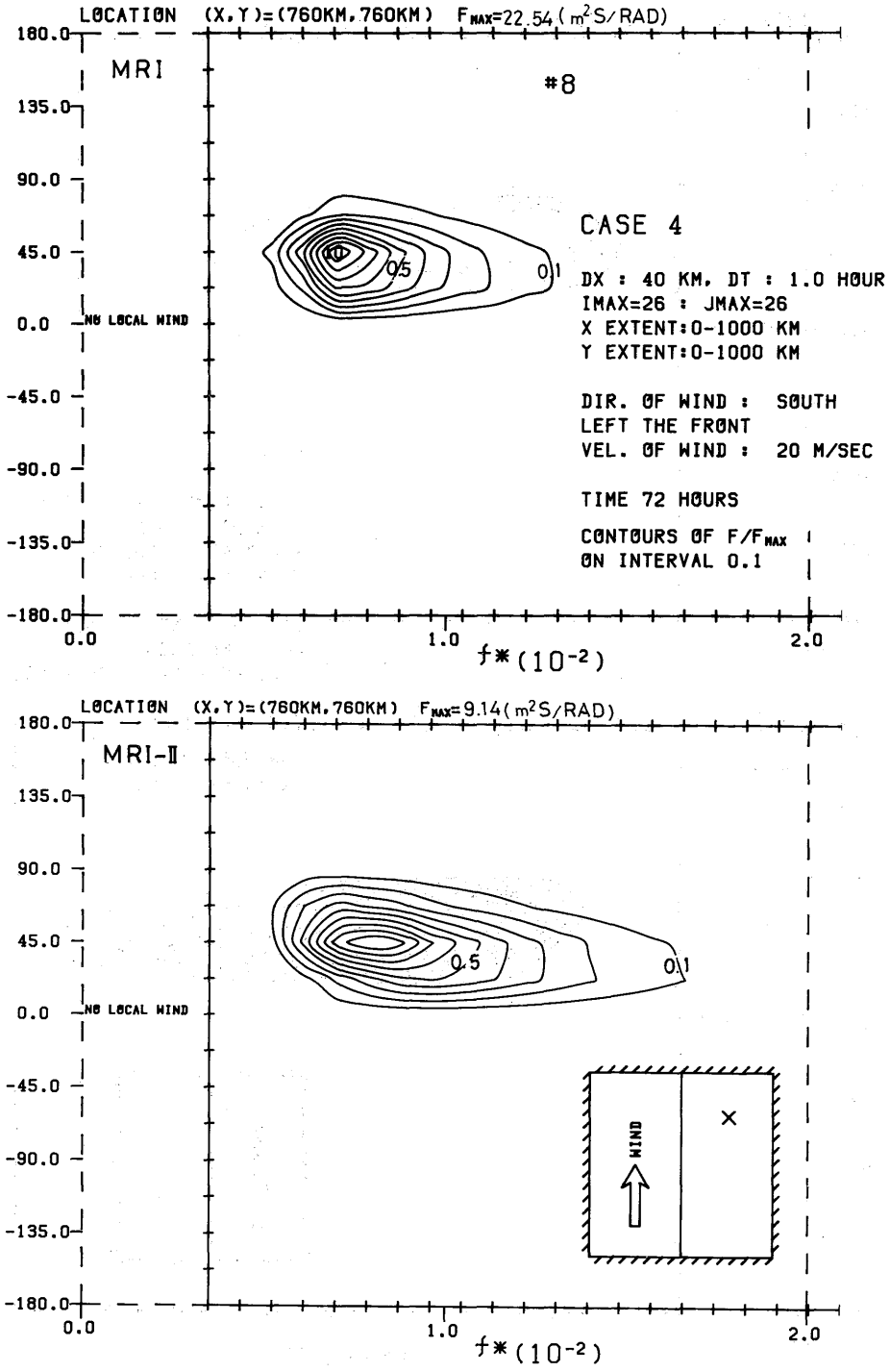

Fig. 62-9.4-23 scaled 2-D spectrum $F(f,\theta)/F(f,\theta)_{MAX}$ for $T = 72$ hrs and point (760,760)

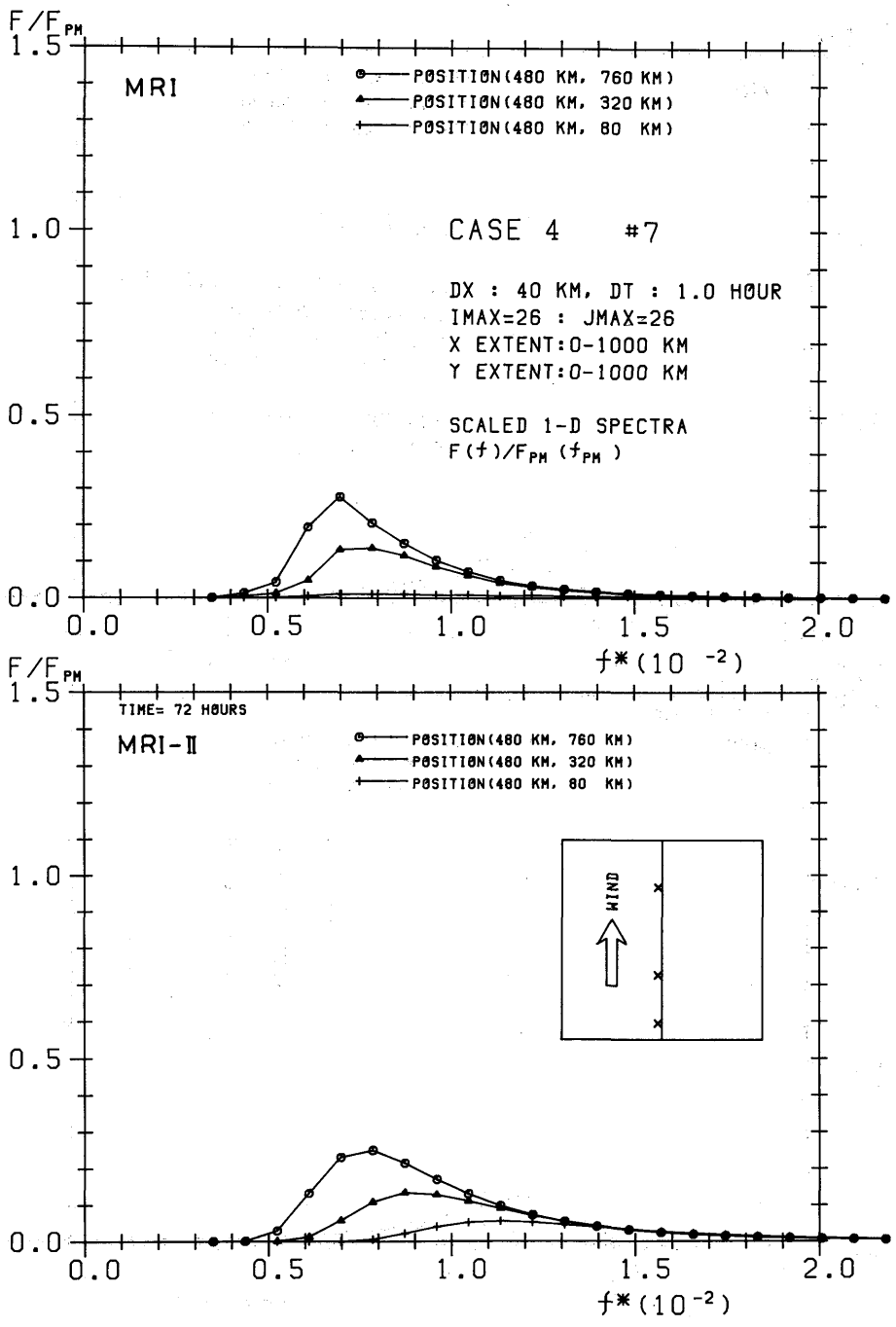

Fig. 63-0-24 scaled 1-D spectrum $F(f)/F(f_{PM})$ for T = 72 hrs and point (480, 80), (480,320) and (480,760)

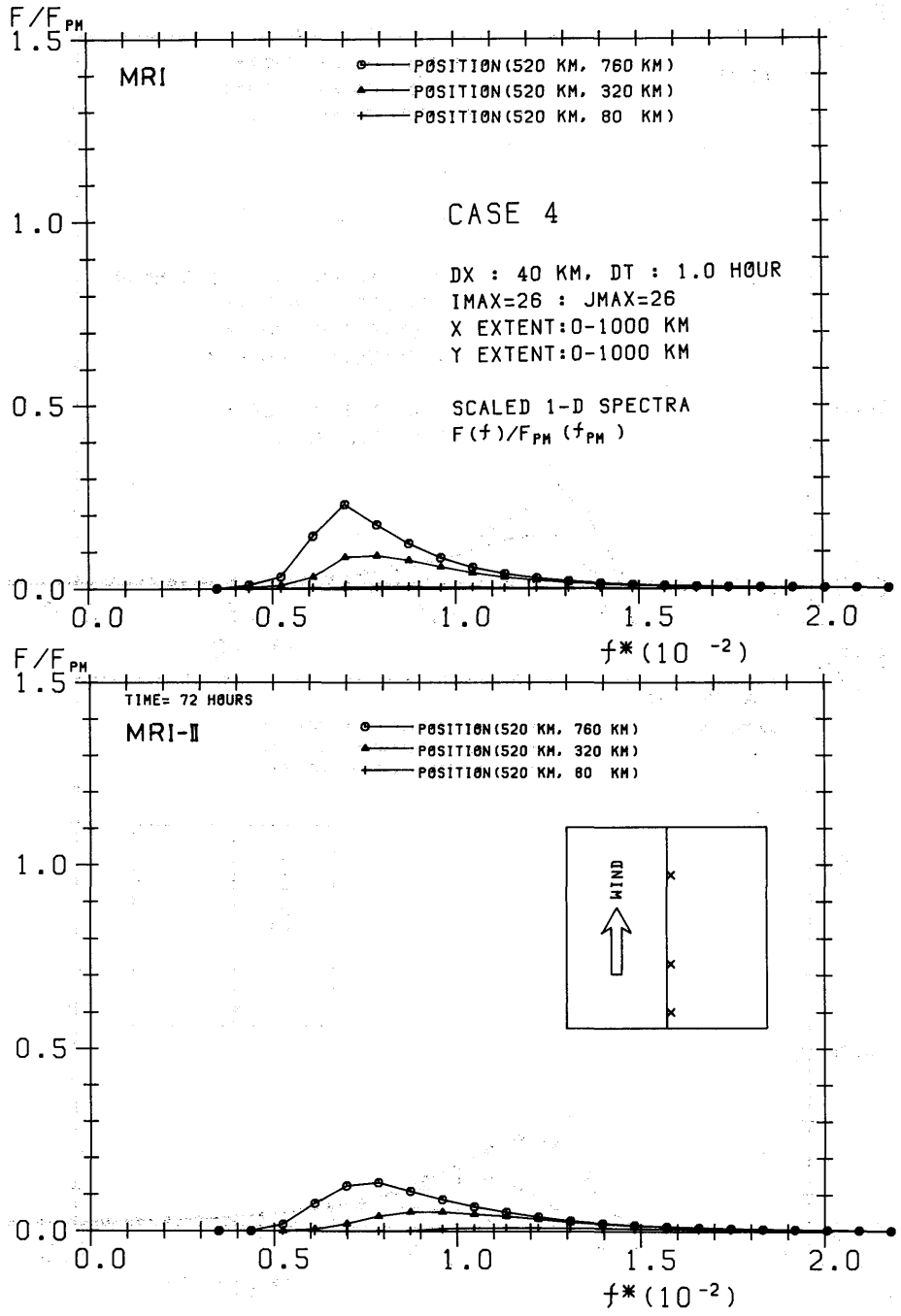

Fig. 64-0-0 scaled 1-D spectrum $F(f)/F(f_{PM})$ for T = 72 hrs and point (520, 80), (520,320) and (520,760)

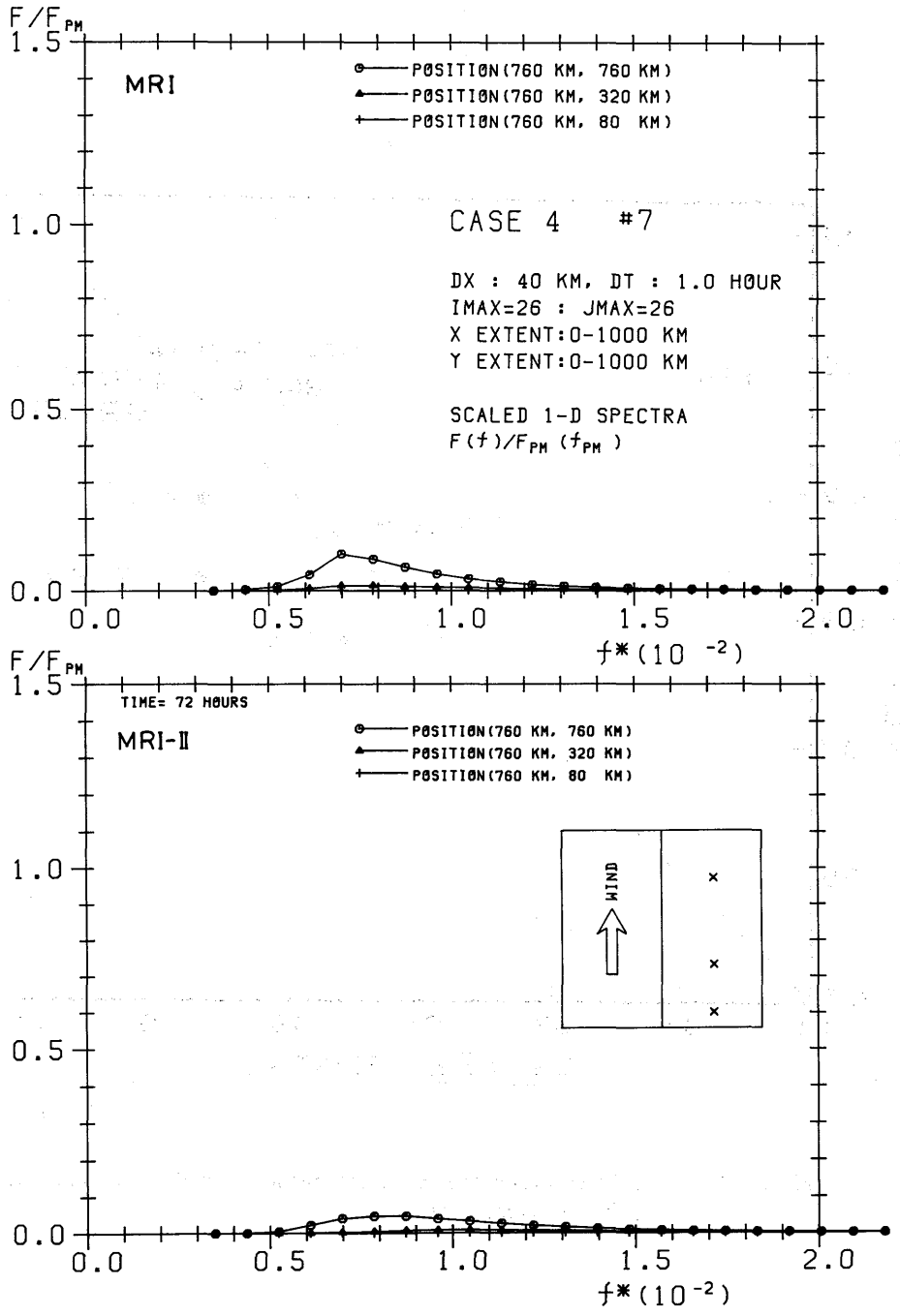

Fig. 65-0-25 scaled 1-D spectrum $F(f)/F(f_{PM})$ for $T = 72$ hrs and point (760, 80), (760,320) and (760,760)

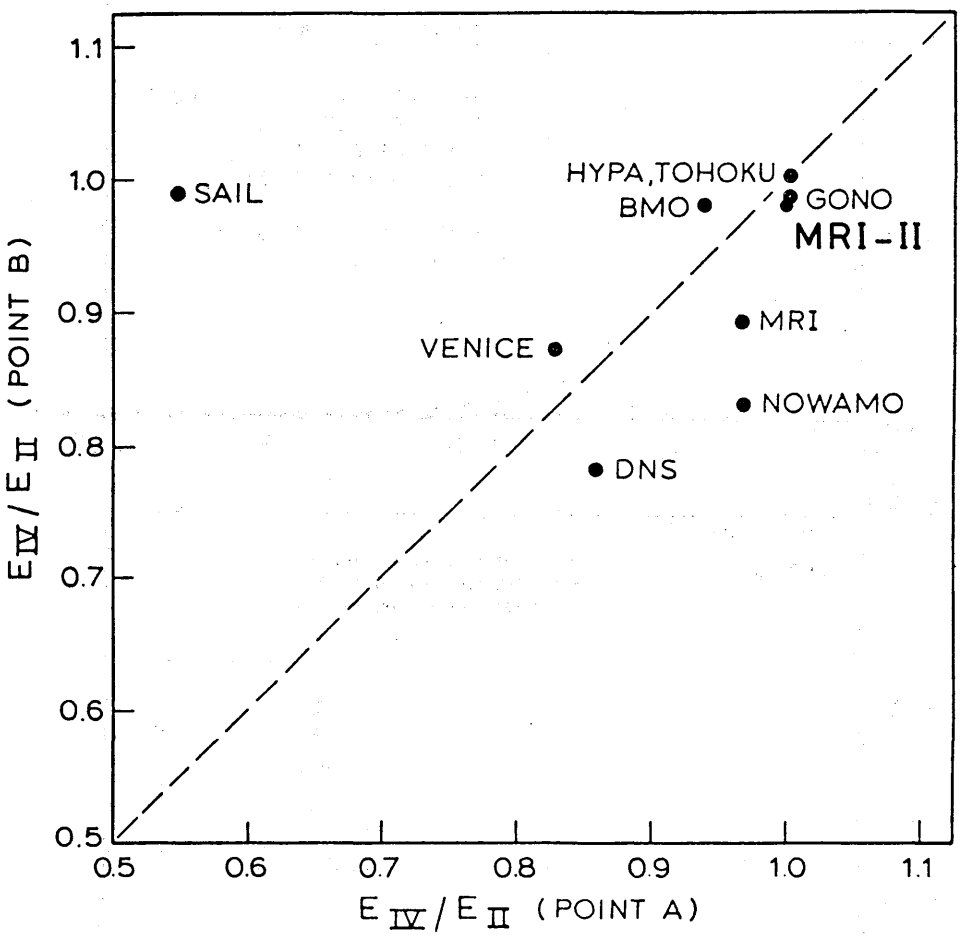

Fig. 66-9.3-0 model locations in the partameter plane spanned by the values of (E_{IV}/E_{II}) at points A and B

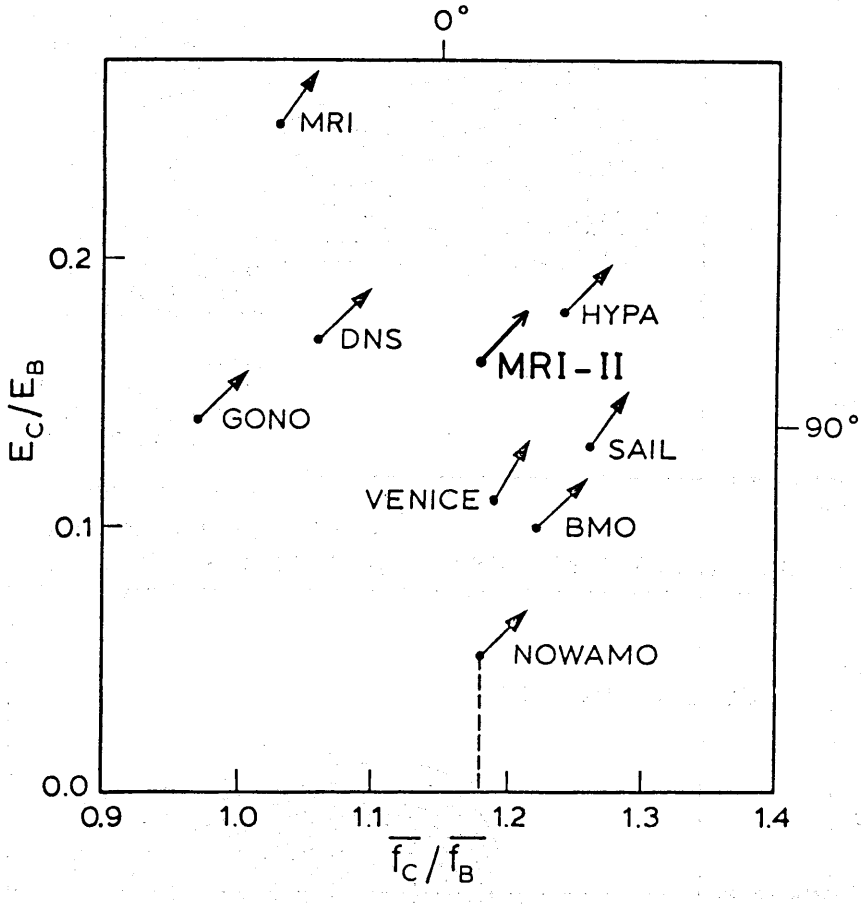

Fig. 67-9.5-0 model locations in the partameter plane of E_C/E_B vs $\bar{f}_C/\bar{f}_B$, where indices B and C refer to points B and C.